Biochemical and Biophysical Research Communications 461 (2015) 186–192

Contents lists available at ScienceDirect

Biochemical and Biophysical Research Communications

journal homepage: www.elsevier.com/locate/ybbrc

Application of GC–MS coupled with chemometrics for scanning serum metabolic biomarkers from renal fibrosis rat

Shao Liu [a, *], Ji-Shi Liu [b], Ren-na Luo [a], Hui Xu [a], Wei-ru Zhang [a], Jie Meng [a], Yi-Zeng Liang [c], Li-Jian Tao [a]

[a] Xiangya Hospital, Central South University, Changsha, Hunan 410008, PR China
[b] Xiangya's Third Affiliated Hospital, Central South University, Changsha, Hunan 410008, PR China
[c] College of Chemistry and Chemical Engineering, Central South University, Changsha, Hunan 410008, PR China

ARTICLE INFO

Article history:
Received 28 March 2015
Available online 13 April 2015

Keywords:
Biomarker
Chemometrics
Gas chromatography–mass spectrometry
Metabolites
Renal fibrosis

ABSTRACT

Renal interstitial fibrosis closely relates to chronic kidney disease and is regarded as the final common pathway in most cases of end-stage renal disease. Metabolomic biomarkers can facilitate early diagnosis and allow better understanding of the pathogenesis underlying renal fibrosis. Gas chromatography–mass spectrometry (GC/MS) is one of the most promising techniques for identification of metabolites. However, the existence of the background, baseline offset, and overlapping peaks makes accurate identification of the metabolites unachievable. In this study, GC/MS coupled with chemometric methods was successfully developed to accurately identify and seek metabolic biomarkers for rats with renal fibrosis. By using these methods, seventy-six metabolites from rat serum were accurately identified and five metabolites (i.e., urea, ornithine, citric acid, galactose, and cholesterol) may be useful as potential biomarkers for renal fibrosis

1. Introduction

Metabolomics, which involves the nontargeted, whole-profiling analysis of the changes of metabolites in cells, tissues, or body fluids, has received increasing interests in recent years [1–5].

Chronic kidney disease (CKD) is a major public health problem worldwide [6–9]. Renal interstitial fibrosis (RIF) closely relates to CKD and is regarded as the final common pathway in most cases of end-stage renal disease [10]. Early diagnosis of RIF contributes to timely treatment. Renal biopsy is, however, the golden standard for diagnosis of RIF. Therefore, to find non-invasive early biomarkers is becoming more and more urgent for risk assessment of RIF.

Unilateral ureteral obstruction (UUO) induces renal fibrosis in rats [11]. The UUO rat model is characterized by renal tubular atrophy, tubular cavity expansion, and interstitial fibrosis, which eventually lead to the structural breakdown and dysfunction of the whole kidney. Screening metabolomic biomarkers can facilitate early diagnosis and allow better understanding of the pathogenesis underlying renal fibrosis in UUO rats. Using 1H NMR-based metabonomics, Zhang et al. studied the metabolic changes of rats with RIF induced by the UUO [12].

Gas chromatography–mass spectrometry (GC/MS) is a robust method for qualitative and quantative analyses of metabolites. Because of its greater sensitivity and separation power than the conventional NMR approach and better reliability in the structure identification of candidate biomarkers than LC/MS, GC/MS has been extensively used in the metabolomics [13–17].

Metabolites in the metabolomic profile of the GC/MS are currently identified and structurally confirmed by comparing samples with standards. Different laboratories run samples at their own equipment, searched MS libraries available, and made structural identifications based on mass spectral data of electron impact (EI) and chemical ionization. Nevertheless, these methods show difficulty in accurately identifying and quantifying metabolites that are co-eluted with, or eluted close to high abundant overloaded metabolites due to overlapping chromatographic peaks [18,19]. In this case, chemometric resolution method may be useful and can be employed to improve the efficiency of metabolomics research.

In this study, the GC/MS coupled with two chemometric resolution methods, heuristic evolving latent projections (HELP) [20,21], and selective ion analysis (SIA) [22–24] was first used to

* Corresponding author. Fax: +86 731 8480 5215.
E-mail addresses: liushao999@hotmail.com (S. Liu), taolj@mail.csu.edu.cn (L.-J. Tao).

http://dx.doi.org/10.1016/j.bbrc.2015.04.031
0006-291X/

investigate metabolites in sera from UUO rats. HELP resolved the partial overlapping chromatographic peaks, and SIA resolved some severely overlapping peaks and embedded peaks. Furthermore, the competitive adaptive reweighted sampling (CARS) method [25] coupled with partial least squares linear discriminant analysis (PLS-LDA) was employed to seek the most potential biomarkers to distinguish UUO rats from the controls.

2. Materials and methods

2.1. Chemicals and reagents

Heptadecanoic acid (98%) (the internal standard), butenedioic acid, oxaloacetic acid,α-oxoglutarate, dodecanic acid, oleic acid, arachidonic acid, aconitic acid, hydroxylamine HCl and N,O-bistrimethylsilyl-trifluoroacetamide (BSTFA) with 1% trimethylchlorosilane (TMCS) were obtained from Sigma–Aldrich (St. Louis, MO, USA). Other chemicals and reagents were purchased from Shanghai Chemicals and Reagents Co. (Shanghai, China).

2.2. Experimental design and sample collection

Specific pathogen-free male Wistar rats (Shanghai Laboratory Animal Center. Shanghai, China), aged 6–8 weeks, were used in the experiment. Animals were housed 4 per cage in rooms maintained at 21 ± 2 °C and 55% relative humidity with alternating 12-h light–dark cycle. Food and water were provided *ad libitum* throughout the experiments. Rats were acclimated to their surroundings over 1 week to eliminate the effect of stress prior to initiation of the experiments. All of the experimental protocols involving animals and their care were carried out according to the regulations of the National Institutes of Health (NIH) of USA and were in compliance with the Institutional Guidelines of the Central South University's.

The experiment included the sham-operated group (SO control group, n = 11) and UUO group (model group, n = 13). The UUO model was established according to the method as described previously [26]. In brief, the left ureter of rats was isolated, exposed, and completely ligated with 4–0 silk suture. The SO group rats underwent an identical surgical intervention except for the ureter ligation. On day 14 after the surgical operation, rats were sacrificed and blood samples was collected from hearts of each rat. Sera were separated from blood samples by centrifugation at 3000 × *g* for 15 min at 4 °C after clot at room temperature for 1 h. Serum samples were stored at −80 °C until required for the GC/MS analysis.

2.3. Sample preparation

A 100 μl of sera was added with 400 μl methanol, and 30 μl heptadecanoic acid as internal standard which was dissolved in methanol at a concentration of 1 mg ml^{-1} . The mixture was then mixed for 1 min and centrifuged for 15 min at 16,000 rpm (17,800× g) at 4 °C. A 400 μl of supernatant was transferred into a 5 ml glass centrifugation tube and evaporated to dryness under a stream of N_2 gas. 50 μl methoxyamine (15 μg/μl) in pyridine was added into residues, and the resultant mixture was mixed for 10 min. Methoxymation was carried out at 70°Cfor 1 h Finally100 μl MSTFA with 1% TMCS was added, mixed for 1 min and heated in a water bath at 60 °C for 45 min before the GC/MS analysis.

2.4. GC/MS conditions

Data were collected on an Agilent 7890A GC with an Agilent 5975C mass selective detector. In the gas chromatographic system, a DB-5 capillary column (30 m, 0.25 mm i.d., film thickness 0.25 mm) was used. Column temperature was held at 100 °C for 3 min, then increased by 8 °C min^{-1} to 300 °C, and held there for 6 min. Inlet temperature was kept at 250 °C. Helium carrier gas was used at a constant flow rate of 1.0 ml min^{-1}. A sample of 1.0 μl was injected with an autoinjector, the split ratio of the injector being 1:10. Mass conditions were as followed: ionization voltage, 70 eV; ion source temperature, 230 °C. Mass data were collected in a full-scan mode (*m*/*z* 50–800). The solvent delay was set at 3.5 min.

2.5. Identification of metabolites

The identification of the metabolites was based on comparison of their mass spectra with NIST08 database or with mass spectra reported in the literature [27–30].

Chemometric resolution methods were employed to recognize and identify overlapping peaks for accurate candidates. Furthermore, the HELP method was utilized for those partially overlapped peaks which had their own selective regions [20,21]. In addition, the SIA method was applied for those seriously overlapped peaks which had not their own selective regions [23]. All computer programs of the HELP and SIA methods used in this study were coded in MATLAB 6.5.

2.6. Data processing and analysis

After sample analysis and metabolites identification, peak areas of 76 metabolites were then extracted to generate a data matrix, in which the rows and columns represented the metabolites and the peak area ratios to the internal standard of the same chromatogram, respectively. Multivariate data analysis was performed using Matlab R2008.a (MathWorks, Inc., MA). Autoscaling, which placed all the measured metabolites on an equal level, was used to preprocess data before multivariate statistical analysis. Principal components analysis (PCA) was used to examine inherent clustering and correlations within the data. CARS method coupled with PLS-LDA [25] was introduced into metabolomics to seek the most probable biomarkers. Statistical significance of the biomarkers was determined by Student's *t*-test. Data with a *P* value of less than 0.05 were considered significant.

3. Results and discussion

3.1. Resulotion of overlapped peaks by HELP

In order to give accurate results, chemometric resolution methods were needed to recognize and identify overlapped peaks.

Representative chromatogram segment in the range of 11.90–12.09 min is shown in Fig. 1A which illustrate the resolution of the overlapping peaks by the HELP method. The HELP method was fully described in previous literature [20,21]. After subtract background and determine the number of components, zero-component and selective regions of the target components by HELP method, pure chromatogram and spectrum were obtained by means of the rank estimation method, and finally three components were resolved in the chromatogram segment of 11.90–12.09 min, and the resolution results are shown in Fig. 1B. Searching with the NIST mass spectral database, components 1 and 2 were provisionally identified as L-methionine(Fig. 1C) and 5-Oxo-proline(Fig. 1D), respectively. Component 3 was not determined due to low similarity indices or because it did not exist in the mass library.

3.2. Resolution of overlapped peaks by SIA

For seriously overlapped peaks which had not selective region in the chromatogram and could not resolved by the HELP method, the

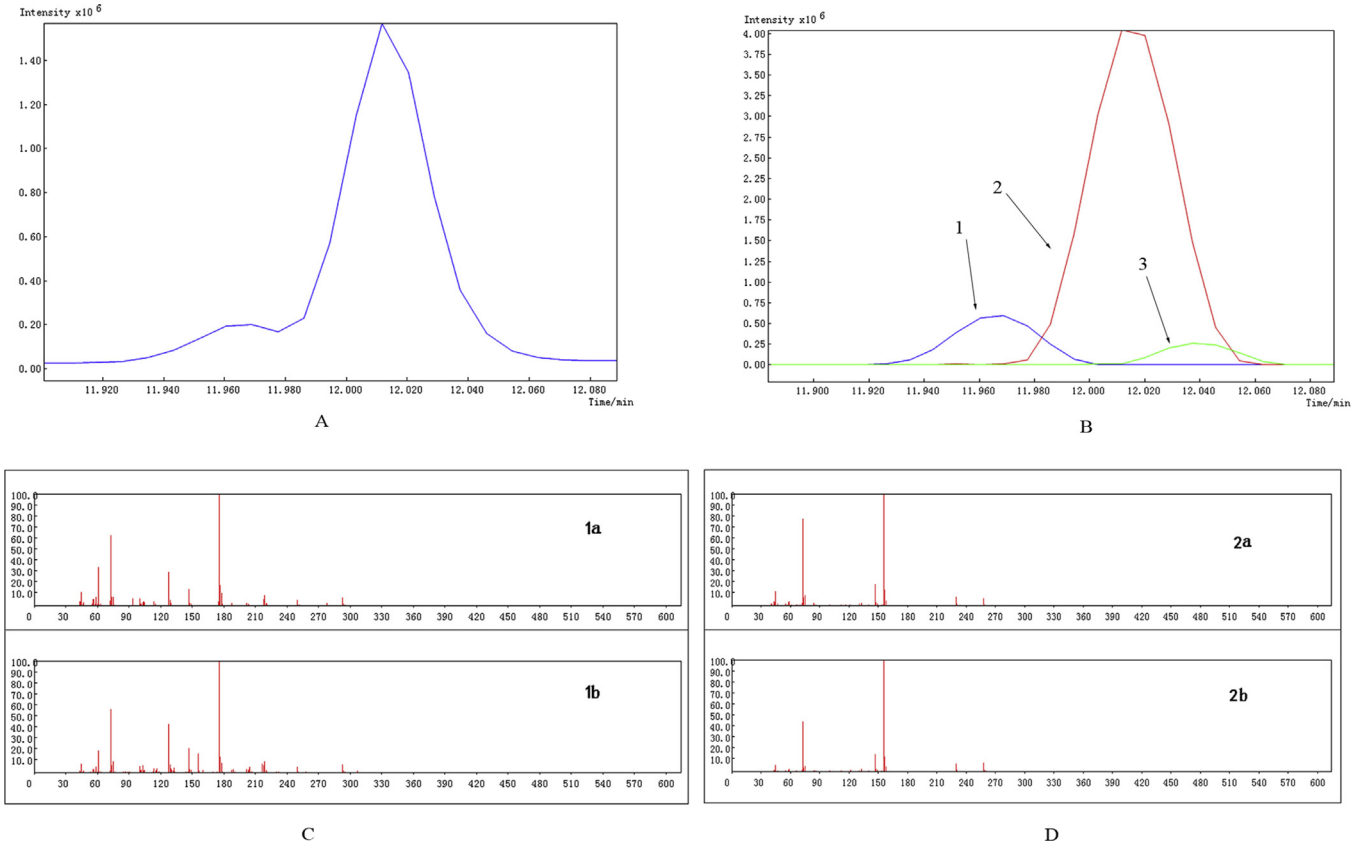

Fig. 1. Resolution of overlapped peaks by HELP. A The total ion chromatogram of the sample within 11.90–12.09 min, B Resolved chromatograms within 11.90–12.09 min containing three components 1, 2 and 3, C The resolved mass spectra of components 1 (1a) and the standard mass spectra of L-methionine (1b), D The resolved mass spectra of components 2 (2a) and the standard mass spectra of 5-Oxo-L-proline (2b).

SIA was introduced because of its high selectivity of mass spectra. A different response at certain *m*/*z* points might be found if a small difference in structure was recognized between the mass spectra of two analytes. Representative chromatogram segment in the range of 21.03–21.17 min is shown to demonstrate how SIA method worked [22–24]. Its original peak cluster and corresponding two-dimensional plot are shown in Fig. 2A and B, respectively. Only one component was seen in the figure. However, the matching index obtained from direct searching with the NIST mass spectral database was as low as about 64%. It suggested that more than one constituent existed in this interval of time. The selective ions of the two components could be found based on the principle of least entropy. The ion at *m*/*z* 202 was the selective ion of the first component, and the ion at *m*/*z* 341 the selective ion of the second component (Fig. 2C). Chromatographic profiles of the two constituents were extracted according to the two selective ions (Fig. 2D). After the pure mass spectra (Fig. 3) were obtained by means of least squares technique, the identification of chemical compounds was performed directly by similarity searches in the NIST mass spectral database. The results showed that components 4 and 5 were identified as tryptophan and octadecanoic acid, respectively.

Other peaks in the test sample were determined by the method as described above. In experimental conditions, glycine, urea, asparagine, lysine, inositol, fructose, galactose and glucose presented two various isomeric forms of TMS derivatives, respectively. Finally, seventy-six metabolites were determined, of which 39 metabolites were confirmed by comparing with standards. The qualitative results of the constituents of the sample are shown in Table 1.

3.3. Pattern recognition and screening potential biomarkers

The patterns of variation in the serum metabolites were analyzed to assess the clustering of SO and UUO groups by using the multivariate statistics from PCA. Superficially, the PCA score plots of the principal components failed to demonstrate distinct clustering or a clear separation of the two groups (Fig. 4A). Thus, the newly proposed CARS method coupled with PLS-LDA was introduced to demonstrate distinct clustering and seek the most probable biomarkers of UUO. CARS, which was based on the simple but effective principle "survival of the fittest" of Darwin's Evolution Theory, was an effective strategy for picking out the key discriminating variables [25]. By using CARS, five metabolites were finally selected, which were urea, ornithine, citric acid, galactose, and cholesterol. A PCA model was reconstructed based on these five metabolites. It was noticable that SO group was distinguished from the UUO group (Fig. 4B). The result indicate these five metabolites may be potential biomarkers. The relative amount of these metabolites was calculated by the integrating area under the peak compared with that under the peak of internal standard (heptadecanoic acid). The quantitative results are shown in Table 2 (data was expressed as the mean ± SD).

Investigators have shown that these metabolites have close relationship with renal disease. Blood urea nitrogen (BUN) is the main terminal product of body protein metabolism and excretes mostly from kidney. Urea filtrates from glomerulus and absorbs at kidney tubules. High protein diets, high catabolism state, water shortage, renal ischemia, insufficient blood volume and kidney damage can raise urea. Though it occurs late in disease progression

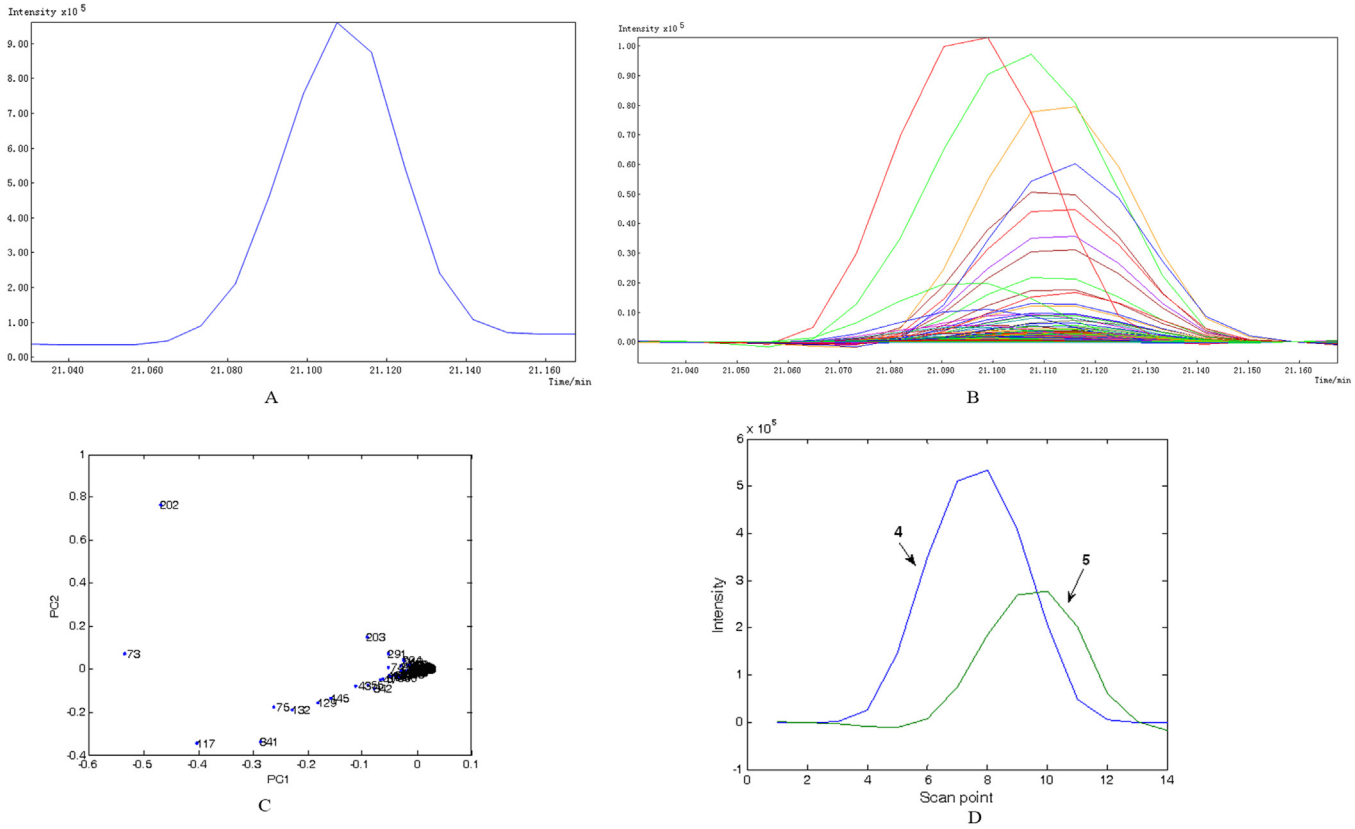

Fig. 2. Resolution of overlapped peaks by SIA. A The total ion chromatogram of the sample within 21.03–21.17 min, B The two-dimension chromatogram of the sample within 21.03–21.17 min, C The selective ion detecting plot, D Resolved chromatograms within 21.03–21.17 min containing three components 4 and 5.

and does not accurately represent the ongoing underlying renal damage, BUN is still current most widely used biomarker for assessing renal function [31]. Ornithine, an alkaline amino acid, plays a role in the urea cycle and has tight relationship with urea [32]. Urea cycle, also called ornithine cycle, is the primary metabolic pathway involved in the clearance of ammonia produced by the breakdown of proteins into urea. Urea cycle not only synthesizes ammonia and CO_2 into urea, but also links urea cycle with citric acid cycle through generating fumaric acid. Any problem in steps of urea cycle will produce diseases. Though disorders of the urea cycle can result from inherited deficiencies or defects of any of eight enzymes, the majority of patients with these disorders are secondary to deficiency of the ornithine. Meanwhile, ornithine is abnormally accumulated in the body in ornithine transcarbamylase deficiency [33]. Citric acid is an important intermediate of the Krebs cycle. Citric acid plays an important role in biological metabolism. Citric acid inhibits development of cataracts, proteinuria and ketosis in streptozotocin (type 1) diabetic rats. Citrate inhibited development of nephropathy (albuminuria) in the diabetic rat and significantly reduced ketonemia in the diabetic rat [34]. Rats with polycystic kidney disease show abnormal renal handling of citrate and ammonia. Citrate salts that have an alkalinizing effect preserve glomerular filtration rate and extend survival [35,36]. Galactose, a normal reducing sugar in the body, has many important biological

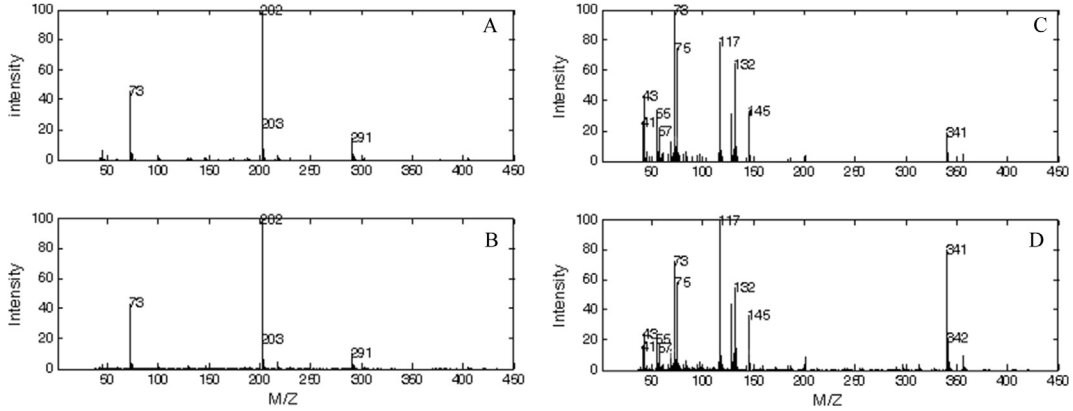

Fig. 3. Resolved mass spectra and their counterpart standard mass spectra. (A) The standard mass spectra of tryptophan, (B) The resolved mass spectra of components 4, (C) The standard mass spectra of octadecanoic acid, (D) The resolved mass spectra of components 5.

Table 1
Metabolites of rat serum as trimethylsilyl (oxime) derivatives using GC–MS coupled with two chemometric resolution methods.

No.	Retention time(min)	Name of compound	Matching index
1	4.20	2 -Hydroxy propanoic acid	96.34%
2	4.84	Alanine[c]	99.11%
3	5.26	2 -Hydroxy butanoic acid	96.02%[a]
4	5.42	Sarcosine(TMS)[c]	90.05%
5	5.82	3 -Hydroxy butanoic acid	98.63%
6	6.83	Valine[c]	97.81%
7	6.26,7.28	Urea	98.50%
8	7.84	Leucine[c]	99.46%
9	7.93	phosphoric acid	99.14%
10	8.23	Isoleucine[c]	99.42%[a]
11	8.29	Proline [c]	94.01%[a]
12	8.39	Malonic acid	91.07%[a]
13	5.11,8.46	Glycine[c]	99.32%[a]
14	8.53	Succinic Acid[c]	96.66%[a]
15	8.93	2,3-Dihydroxy propanoic acid	98.56%
16	9.01	pyrimidine	98.10%[a]
17	9.18	2,3-Dihydroxybutanoic acid	98.82%[a]
18	9.43	Serine[c]	95.08%
19	9.93	Threonine[c]	92.83%
20	11.25	Aminomalonic acid	99.17%[a]
21	11.29	Aspartic acid[c]	90.63%[a]
22	11.55	Malic acid3[c]	97.81%
23	11.96	Methionine[c]	97.38%[a]
24	12.03	5-Oxo- proline	97.09%[a]
25	12.13	4- Hydroxy proline	98.99%
26	12.52	Oxaloacetic acid[c]	96.17%[a]
27	12.58	Creatinine[c]	96.88%
28	12.78	2,3,4-Trihydroxybutyric acid	97.47%[a]
29	12.87	2-(Methoxyimino)-Pentane dioic acid	98.22%
30	13.34	α-oxoglutarate[c]	90.13%
31	13.43,16.29	Ornithine[c]	99.37%
32	13.51	Glutamate[c]	99.05%
33	13.61	Phenylalanine[c]	99.63%
34	13.74,14.27	Asparagine	95.38%
35	13.81	Dodecanic acid[c]	92.23%
36	14.55	Xylose	98.71%
37	14.75,17.62	Lysine[c]	98.51%
38	15.13	Ribitol[c]	97.86%
39	15.34	Aconitic acid[c]	89.54%[a]
40	15.67	Glutamine[c]	97.48%
41	16.06	N-benzoyl-glycine	95.54%
42	16.38	Citric Acid[c]	93.29%
43	16.49	Tetradecoic acid [c]	93.49%
44	16.55	Ribose	96.62%
45	16.66,16.81	Fructose[c]	95.26%
46	16.90,17.20	Galactose[c]	95.84%
47	17.28	Alloxanoic acid	93.33%
48	17.38	Glucitol[c]	96.32%
49	17.41	Galactopyronose[c]	99.53%
50	17.58	Histidine[c]	93.04%[b]
51	17.56,17.77	Glucose[b,c]	96.81%
52	17.83	Tyrosine[c]	95.71%
53	17.93	Mannitol	93.44%
54	18.03	Gluconic acid	92.86%
55	18.19	Mannonic acid lactone	97.86%
56	18.33	Xylofuranose	97.81%
57	18.48	Xylonic acid lactone	98.61%[b]
58	18.50	Glucopyranose	91.55%[b]
59	18.67	Palmitelaidic acid	99.01%
60	18.85	Altronic acid	94.07%
61	18.91	palmitic acid[c]	97.63%
62	19.48	1H-Indole-3-propanoic acid	96.29%
63	18.23,19.82	Inositol	97.54%
64	19.88	uric acid	98.37%
65	20.80	9,12-Octadecadienoic acid	97.05%
66	20.85	Oleic acid[c]	98.24%
67	20.92	11- octadecenoic acid	96.34%
68	21.09	L-tryptophan[c]	99.17%[b]
69	21.12	Octadecanoic acid[c]	99.01%[b]
70	21.92	Glucose phosphate[c]	95.30%
71	22.48	Arachidonic acid[c]	97.11%
72	22.75	Hexanedioic,bis (2-ethylhexyl) ester	98.67%
73	23.42	Myo-Inositol phosphate	92.02%
74	29.71	Cholesterol [c]	98.04%
75	31.14	campesterol[c]	95.00%
76	32.35	β-sitosterol[c]	94.20%

[a] The peak was resolved by HELP.
[b] The peak was resolved by SIA.
[c] The peak was confirmed by comparing with samples of standards.

functions and imbalance of it will cause diseases. At the normal level, it is usually converted into glucose by galactose-1-phosphate uridyltransferase and galactokinase. At the high level, it will cause accumulation of ROS, or stimulate free radical aproduction indirectly by the formation of advanced glycation end products (AGEs) *in vivo*, finally resulting in oxidative stress [37,38]. Galactose is also an essential basic substrate for biosynthesis of many macromolecules in the body. Leptin [39] and b3-adrenergic receptor agonists [40] can reduce absorption of galactose and aldose reductase can enhance the breakdown of galactose by catalyzing the NADPH-mediated conversion of galactose to galactitol. The latter pathway is very important in galactose toxicity via accumulation of galactitol. Cholesterol, a multi-cyclopentane hydrogen of the derivatives, have a strong correlation with renal dysfunction [41,42]. Renal cholesterol crystal embolization, also known as atheroembolic renal disease, is caused by showers of cholesterol crystals from an atherosclerotic aorta that occludes small renal arteries. Cholesterol crystal embolism may give rise to different degrees of renal impairment [43]. Many researchers nowadays are with a view to make clear relationship between lipids and renal dysfunction. Cholesterol lies in the blood in form of lipoprotein cholesterol (LDL-C). LDL-C level is associated with atherosclerosis and fibrosis in different organs [44–46].

These five metabolites have their own important role in biological metabolisms. Simultaneously, they tightly relate to each other and involve in energy metabolism. Abnormal of urea, ornithine, citric acid, galactose and cholesterol in serum of UUO rats may be an early information of renal injury.

4. Conclusions

Application of metabolic profiles is significantly useful to discover informative biomarkers which are predictive of a clinical outcome under investigation. Therefore, the metabolomic research shall involve comprehensive analyses of metabolites from body fluids. In the present study, the GC/MS combined with chemometric methods, for the first time, were employed to identify the constituents in sera of rats. The results showed that the HELP and SIA methods effectively recognized overlapping peaks of GC/MS data, and a total of 76 metabolites were identified. By using CARS, five metabolites were finally selected. These five metabolites quantatively distinguished the diseased condition of UUO rats from control rats, which supported that the five metabolites might be useful as potential biomarkers. Therefore, this well-developed new method will be a promising and efficient tool to seek the most potential biomarkers useful for distinguishing the rats with UUO-induced renal fibrosis from the control. It is worthwhile noting that the pathogenesis of renal fibrosis is complex and complicated; therefore, the investigation different animal models resembling renal firobsis will be able to determine comprehensive changes of metabolites as possible as it can.

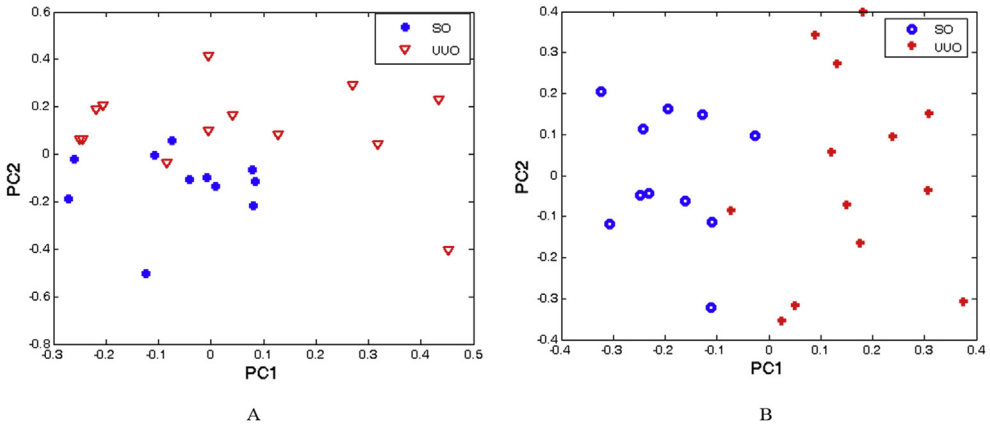

Fig. 4. PCA score plot based on the metabolites. A PCA score plot based on the all metabolites from the serum samples, (SO, represents sham-operated controls group; UUO, represents Unilateral ureteral obstruction model group), B PCA score plot based on the five metabolites from the serum samples, (SO, represents sham-operated controls group; UUO, represents Unilateral ureteral obstruction model group).

Table 2
The relative concentrations of Urea, Ornithine, Citric Acid, Galactose and Cholesterol.

Metabolites	SO group concentration(ng/ul)	UUO group concentration(ng/ul)
Urea	517.48 ± 108.11	702.78 ± 149.09
Ornithine	11.99 ± 2.22	16.88 ± 3.85
Citric Acid	12.52 ± 2.69	17.30 ± 4.62
Galactose	1.41 ± 0.58	0.55 ± 0.35*
Cholesterol	113.65 ± 28.94	157.85 ± 26.52

Concentration values shown are mean ± SD of ratio to I.S.
P value of <0.05 was considered statistically significant and signed '*'.

Conflict of interest

None.

Acknowledgments

The authors thank Prof. Xiong Cai (Hunan University of Chinese Medicine) for critical review of the manuscript. This work was supported by the Natural Science Fund of Hunan Province of China (13JJ3017).

Transparency document

Transparency document related to this article can be found online at http://dx.doi.org/10.1016/j.bbrc.2015.04.031.

References

[1] J.T. Brindle, H. Antti, E. Holmes, G. Tranter, J.K. Nicholson, H.W.L. Bethell, S. Clarke, P.M. Schofield, E. Mckilligin, D.E. Mosedale, D.J. Grainger, Rapid and noninvasive diagnosis of the presence and severity of coronary heart disease using H-1-NMR-based metabonomics, Nat. Med. 8 (2002) 1439–1444.
[2] H.C. Gao, B.J. Dong, X. Liu, H.Q. Xuan, Y.R. Huang, D.H. Lin, Metabonomic profiling of renal cell carcinoma: high-resolution proton nuclear magnetic resonance spectroscopy of human serum with multivariate data analysis, Anal. Chim. Acta 624 (2008) 269–277.
[3] W. Silvia, S. Karoline, S. Maximilian, K. Marco, V. Wolfgang, Tools in metabonomics: an integrated validation approach for LC-MS metabolic profiling of Mercapturic acids in human urine, Anal. Chem. 79 (2007) 2918–2926.
[4] A. Sreekumar, L.M. Poisson, T.M. Rajendiran, A.P. Khan, Q. Cao, J. Yu, B. Laxman, R. Mehra, R.J. Lonigro, Y. Li, M.K. Nyati, A. Ahsan, S. Kalyana-Sundaram, B. Han, X. Cao, J. Byun, G.S. Omenn, D. Ghosh, S. Pennathur, D.C. Alexander, A. Berger, J.R. Shuster, J.T. Wei, S. Varambally, C. Beecher, A.M. Chinnaiyan, Metabolomic profiles delineate potential role for sarcosine in prostate cancer progression, Nature 457 (2009) 910–914.
[5] R.Y. Xue, Z.X. Lin, C.H. Deng, L. Dong, T.T. Liu, J.Y. Wang, X.Z. Shen, A serum metabolomic investigation on hepatocellular carcinoma patients by chemical derivatization followed by gas chromatogrphy-mass spectrometry, Rapid Commun. Mass Spectrom. 22 (2008) 3061–3068.
[6] J. Coresh, E. Selvin, L.A. Stevens, J. Manzi, J.W. Kusek, P. Eggers, L.F. Van, A.S. Levey, Prevalence of chronic kidney disease in the United States, JAMA 298 (2007) 2038–2047.
[7] S.E. Baumeister, C.A. Böger, B.K. Krämer, A. Döring, D. Eheberg, B. Fischer, J. John, W. Koenig, C. Meisinger, Effect of chronic kidney disease and comorbid conditions on health care costs: a 10-Year observational study in a general population, Am. J. Nephrol. 31 (2010) 222–229.
[8] E.I.N.A. Meguid, A.K. Bello, Chronic kidney disease: the global challenge, Lancet 365 (2005) 331–340.
[9] J. Coresh, B.C. Astor, T. Greene, G. Eknoyan, A.S. Levey, Prevalence of chronic kidney disease and decreased kidney function in the adult US population: Third National Health and Nutrition Examination Survey, Am. J. Kidney Dis. 41 (2003) 1–12.
[10] A.A. Eddy, Molecular basis of renal fibrosis, Pediatr. Nephrol. 15 (2000) 290–301.
[11] R.L. Chevalier, M.S. Forbes, B.A. Thornhill, Ureteral obstruction as a model of renal interstitial fibrosis and obstructive nephropathy, Kidney Int. 75 (2009) 1145–1152.
[12] H.Y. Zhang, J.M. Jia, J.G. Cheng, F.Q. Ye, X.K. Li, H.C. Gao, ^{1}H NMR-based metabonomics study on serum of renal interstitialfibrosis rats induced by unilateral ureteral obstruction, Mol. Biosyst. 8 (2012) 595–601.
[13] M.M. Zeng, Z.H. Che, Y.Z. Liang, B. Wang, X. Chen, H.D. Li, J.H. Deng, Z.G. Zhou, GC–MS based plasma metabolic profiling of type 2 diabetes mellitus, Chromatographia 69 (2009) 941–948.
[14] J. Lin, M. Su, X. Wang, Y. Qiu, H. Li, J. Hao, H. Yang, M. Zhou, C. Yan, W. Jia, Multiparametric analysis of amino acids and organic acids in rat brain tissues using GC/MS, J. Sep. Sci. 31 (2008) 2831–2838.
[15] Q. Zhang, G. Wang, Y. Du, L. Zhu, J. An, GC/MS analysis of the rat urine for metabonomic research, J. Chromatogr. B 854 (2007) 20–25.
[16] X. Tao, Y. Liu, Y. Wang, Y. Qiu, J. Lin, A. Zhao, M. Su, W. Jia, GC–MS with ethylchloroformate derivatization for comprehensive analysis of metabolites in serum and its application to human uremia, Anal. Bioanal. Chem. 391 (2008) 2881–2889.
[17] Y. Qiu, M. Su, Y. Liu, M. Chen, J. Gu, J. Zhang, W. Jia, Application of ethyl-chloroformate derivatization for gas chromatography–mass spectrometry based metabonomic profiling, Anal. Chim. Acta (2007) 277–283.
[18] J. Van-Der-Greef, P. Stroobant, R. Van-Der-Heijden, The role of analytical sciences medical systems biology, Curr. Opin. Chem. Biol. 8((2004) 559–565.
[19] H. Kanani, P.K. Chrysanthopoulos, M.I. Klapa, Standardizing GC–MS metabolomics, J. Chromatogr. B 871 (2008) 91–201.
[20] Y.Z. Liang, O.M. Kvalheim, H.R. Keller, Heuristic evolving latent projections: resolving two-way multicomponent data. 2. Detection and resolution of minor constituents, Anal. Chem. 64 (1992) 946–953.
[21] O.M. Kvalheim, Y.Z. Liang, Heuristic evolving latent projections: resolving two-way multicomponent data. 1. Selectivity, latent-projective graph, datascope, local rank, and unique resolution, Anal. Chem. 64 (1992) 936–946.
[22] M. Wang, Y.H. Xiong, M.M. Zeng, H.D. Li, T.M. Zhang, Y.Z. Liang, GC-MS combined with chemometrics for analysis of the components of the essential oils of sweet potato leaves, Chromatographia 71 (2010) 891–897.
[23] B.B. Tan, Y.Z. Liang, L.Z. Yi, H.D. Li, Z.G. Zhou, X.Y. Ji, J.H. Deng, Identification of free fatty acids profiling of type 2 diabetes mellitus and exploring possible biomarkers by GC–MS coupled with chemometrics, Metabolomics 6 (2010) 219–228.

[24] X.N. Xu, Z.H. Tang, Y.Z. Liang, Comparative analysis of plant essential oils by GC–MS coupled with integrated chemometric resolution methods, Anal. Methods 2 (2010) 359–367.
[25] H.D. Li, Y.Z. Liang, Q.S. Xu, D.S. Cao, Key wavelengths screening using competitive adaptive reweighted sampling method for multivariate calibration, Anal. Chim. Acta 648 (2009) 77–84.
[26] M. Satoh, N. Kashihara, Y. Yamasaki, K. Maruyama, K. Okamoto, Y. Maeshima, Renal interstitial fibrosis is reduced in angiotensin II type 1a receptor-deficient mice, J. Am. Soc. Nephrol. 12 (2001) 317–325.
[27] H. Wu, R.Y. Xue, L. Dong, T.T. Liu, C.H. Deng, H.Z. Zeng, X.Z. Shen, Metabolomic profiling of human urine in hepatocellular carcinoma patients using gas chromatography/mass spectrometry, Anal. Chim. Acta 648 (2009) 98–104.
[28] T. Shepherda, G. Dobson, S.R. Verrall, S. Conner, D.W. Griffiths, J.W. Nicol, H.V. Davies, D. Stewart, Potato metabolomics by GC–MS: what are the limiting factors? Metabolomics 3 (2007) 475–488.
[29] D.R. Rudell, J.P. Mattheis, E.A. Curry, Prestorage ultraviolet-White light irradiation alters apple peel metabolome, J. Agric. Food Chem. 56 (2008) 1138–1147.
[30] M. Cocchi, C. Durante, M. Grandi, P. Lambertini, D. Manzini, A. Marchetti, Simultaneous determination of sugars and organic acids in aged vinegars and chemometric data analysis, Talanta 69 (2006) 1166–1175.
[31] C.G. Duarte, H.G. Preuss, Assessment of renal function–glomerular and tubular, Clin. Lab. Med. 13 (1993) 33–52.
[32] F.M.V. Kloet, I. Bobeldijk, E.R. Verheij, R.H. Jellema, Analytical error reduction using single point calibration for accurate and precise metabolomic phenotyping research articles, J. Proteome Res. 8 (2009) 5132–5141.
[33] M. Tuchman, B. Lee, U. Lichter-Konecki, M.L. Summar, M. Yudkoff, S.D. Cederbaum, D.S. Kerr, G.A. Diaz, M.R. Seashore, H.S. Lee, R.J.M. Carter, J.P. Krischer, M.L. Batshaw, Cross-sectional multicenter study of patients with urea cycle disorders in the United States, Mol. Genet. Metab. 94 (2008) 397–402.
[34] R. Nagai, M. Nagai, S. Shimasaki, J.W. Baynes, F. Yukio, Citric acid inhibits development of cataracts, proteinuria and ketosis in streptozotocin (type 1) diabetic rats, Biochem. Biophys. Res. Commun. 393 (2010) 118–122.
[35] G.A. Tanner, J.A. Tanner, Citrate therapy for polycystic kidney disease in rats, Kidney Int. 58 (2000) 1859–1869.
[36] G.A. Tanner, Potassium citrate/citric acid intake improves renal function in rats with polycystic kidney disease, J. Am. Soc. Nephrol. 9 (1998) 1242–1248.
[37] Q. Zhang, X. Li, X. Cui, P. Zuo, D-galactose injured neurogenesis in the hippocampus of adult mice, Neurol. Res. 27 (2005) 552–556.
[38] X. Hua, M. Lei, Y. Zhang, J. Ding, Q. Han, G. Hu, M. Xiao, Long-term D-galactose injection combined with ovariectomy serves as a new rodent model for Alzheimer's disease, Life Sci. 80 (2007) 1897–1905.
[39] M.P. Lostao, E. Urdaneta, E.A. Martinez, A. Barber, J.A. Martinez, Presence of leptin receptors in rat small intestine and leptin effect on sugar absorption, FEBS Lett. 423 (1998) 302–306.
[40] A.S. Diez, F.I. Milagro, B. Berraondo, M.A. Zulet, J.A. Martinez, A. Barber, Effects of trecadrine, a beta 3-adrenergic agonist, on intestinal absorption of D-galactose and disaccharidase activities in three physiopathological models, J. Pharm. Pharmacol. 49 (1997) 873–877.
[41] S.S. Elke, K. Tobias, C.C. Gary, J.G. Robert, M.R. Kathryn, B. Colin, E.B. Julie, G. Michael, Cholesterol and the risk of renal dysfunction in apparently healthy men, J. Am. Soc. Nephrol. 14 (2003) 2084–2091.
[42] T. Hirano, Abnormal lipoprotein metabolism in CKD, Nihon Jinzo Gakkai Shi 55 (2013) 1276–1279.
[43] F. Scolari, R. Tardanico, R. Zani, A. Pola, B.F. Viola, E. Movilli, R. Maiorca, Cholesterol crystal embolism: a recognizable cause of renal disease, Am. J. Kidney Dis. 36 (2000) 1089–1109.
[44] C.D. Gardner, S.P. Fortmann, R.M. Krauss, Association of small low-density lipoprotein particles with the incidence of coronary artery disease in men and women, JAMA 276 (1996) 875–881.
[45] A. Acay, F. Erdenen, E. Altunoglu, H. Erman, C. Muderrisoglu, G.G. Korkmaz, R. Gelisgen, O. Tabak, H. Uzun, Evaluation of serum paraoxonase and arylesterase activities in subjects with asthma and chronic obstructive lung disease, Clin. Lab. 59 (2013) 1331–1337.
[46] T. Bulum, B. Kolarić, I. Prkacin, L. Duvnjak, Total and LDL cholesterol are associated with glomerular filtration rate in normoalbuminuric type 1 diabetic patients, Coll. Antropol. 37 (2013) 771–776.